Structure and substructure in the stellar halo of the Milky Way
Pila Diez, B.

Author: Pila Díez, Berenice
Title: Structure and substructure in the stellar halo of the Milky Way
Issue Date: 2015-06-16

Chapter 6

Search for halo substructure in KiDS

Authors

B. Pila-Díez, J.T.A. de Jong, K. Kuijken and the KiDS consortium

Abstract

We use data from the data release 1 and data release 2 from the Kilo Degree Survey, a public survey at the ESO VLT Survey Telescope, to map the halo using near main sequence stars and red clump stars. We search for stellar overdensities at different distance or magnitude ranges, aiming to detect new satellites or tidal debris. We recover broad structures like the Sagittarius stream (both in the northern and in the southern hemisphere), the Eastern Band Structure, the Virgo Overdensity and part of the Galactic disk, and we also identify a piece of the Palomar 5 tails. Using Colour Magnitude Diagrams and derived stellar density maps, we test several candidate narrow overdensities for both colour-magnitude and spatial coherence, but conclude that none of the candidates is a real satellite or a piece of cold accreted substructure.

6.1 Introduction

The search for satellites and for tidal remnants is one of the main goals of Galactic halo studies, since they provide a look both into the current accretion history of the Galaxy and into the star formation history of the satellite or the progenitor. They can also provide constraints on the mass and shape of the dark matter halo. Additionally they help set constraints on the Λ-Cold Dark Matter cosmological model and serve as a test bench for its predictions.

In the last decade, many satellite galaxies have been discovered, and the first cold stellar streams in the halo of the Galaxy have been revealed. This has been possible thanks to the advent of deep multi-colour large area surveys such as 2MASS, SDSS, Pan-STARRS, DES and others. 2MASS was particularly successful in tracing with red giant stars the two tails of the Sagittarius stellar stream wrapping at least 180 deg each around the galaxy (Majewski et al. 2003). SDSS has uncovered a wealth of new satellite galaxies (Belokurov et al. 2007c; Zucker et al. 2006) and a myriad of streams, associated both to dwarf galaxies (Belokurov et al. 2006b; Grillmair 2006a; Newberg et al. 2010) and to globular clusters (Odenkirchen et al. 2001; Grillmair & Dionatos 2006a; Grillmair & Johnson 2006). Pan-STARRS, on the other hand, has discovered one thin cold stream (Bernard et al. 2014). And the PAndAS survey —which targeted M31's halo— has probed at least five stellar structures in the Milky Way's halo along the line of sight to the Andromeda galaxy: the Monoceros ring, the Pisces/Triangulum globular cluster stream and three structures possibly associated to the Triangulum/Andromeda overdensity (Martin et al. 2014). Most recently, DES has reported the discovery of 9 new satellites in the Southern sky (The DES Collaboration et al. 2015; Koposov et al. 2015), and last year ATLAS also unveiled a new stream in the Southern sky (Koposov et al. 2014).

The Kilo Degree Survey (KiDS), is one of three public surveys currently underway on the ESO VLT Survey Telescope (VST). It is designed to map the large scale dark matter distribution through weak gravitational lensing, and is currently scanning the sky to cover 1500 deg^2 to a depth approximately 2 magnitudes fainter than SDSS. Most of the planned footprint of KiDS targets the Southern hemisphere of the sky which, for logistic reasons, has not been as extensively surveyed as the Northern hemisphere thus far. Ongoing surveys in the South—such as KiDS itself but also ATLAS and DES—are now reporting first results. With the first data releases, KiDS DR-1 and DR-2, now available, it is time to start testing the data set and explore the halo for signs of substructure.

In this chapter we briefly review the observations, survey strategy and data processing of KiDS (section 6.2), describe the techniques we have used to search for new substructure (section 6.3.1), present recovered substructures and candidate overdensities (section 6.3.2) and discuss our results as well as the future prospects (section 6.4). Finally we summarize the main ideas of the work in section 6.5.

6.2 Observations and data processing

The Kilo Degree Survey (de Jong et al. 2013, KiDS) is an optical broad-band multi-filter survey (u, g, r, and i) with the VST, imaging 1500 $\deg^2$ over a northern and a southern field. The field of view of its individual pointings is $1 \times 1 \deg^2$ with an image quality between $0.7''$ for the r band and $1.1''$ for the u band (PSF FWHM). It reaches limiting magnitudes of 24.3 in u, 25.1 in g, 24.9 in r and 23.7 in i, making it 1.5 to 2.0 magnitudes deeper than SDSS or ATLAS.

In this work we use the images from the first and second public data releases (DR), a total of 148 square degrees. The sky footprint for these DR-1 and DR-2 images is shown in Fig.6.1.

The PSF is homogenized across each image in order to be able to obtain accurate shapes, PSF-corrected matched-aperture photometry, improved colours and a refined star-galaxy separation. We produce photometric catalogues using the "Gaussian Aperture and PSF" (GAaP) code described in section 2.1 of chapter 3, and use the flux ratio between two apertures in the r band ($0.5''$ and $0.7''$) to separate (Gaussian) stars from (more extended) galaxies. We correct for interstellar extinction using the Schlegel et al. (1998) dust maps and we cut the source catalogues at a magnitude limit of $r < 23.2$ mag to avoid small, round, faint galaxies. Finally, we correct the photometry for a seeing-dependency and transform the KiDS magnitudes to the SDSS system.

Finally, from these catalogues we select near main sequence turnoff point (nearMSTO) stars, red clump (RC) stars and blue horizontal branch (BHB) stars following the prescriptions in Pila-Díez et al. (2015) (chapter 2), Correnti et al. (2010) and Belokurov et al. (2014) (after Yanny et al. (2000) and Deason et al. (2011)), respectively. We note that the RC sample may suffer contamination from K0-K2 main sequence field stars, and may be locally enhanced if a main sequence overdensity is present. This precludes us from directly inferring distances for the RC sample but, nonetheless, it does not prevent us from using the sample in search for spatially localized overdensities in the apparent magnitude space.

More details on the survey, on the data processing, on the production of the stellar catalogues and on the photometric transformations described above can be found in chapter 3.

6.3 Search for overdensities

6.3.1 Methodology

We use the nearMSTO, the RC and the BHB stars catalogues to build stellar maps and stellar density maps for different distance or magnitude ranges. The BHB maps result in very few counts with no clear overdensities, so we do not use them further. On the other hand, the nearMSTO and the RC maps return sufficiently populated maps to be used in the search for spatial enhancements. The distance-sliced stellar and stellar density maps for the nearMSTO stars in the different KiDS fields are shown in figures 6.6 to 6.9. We present the star density in eight

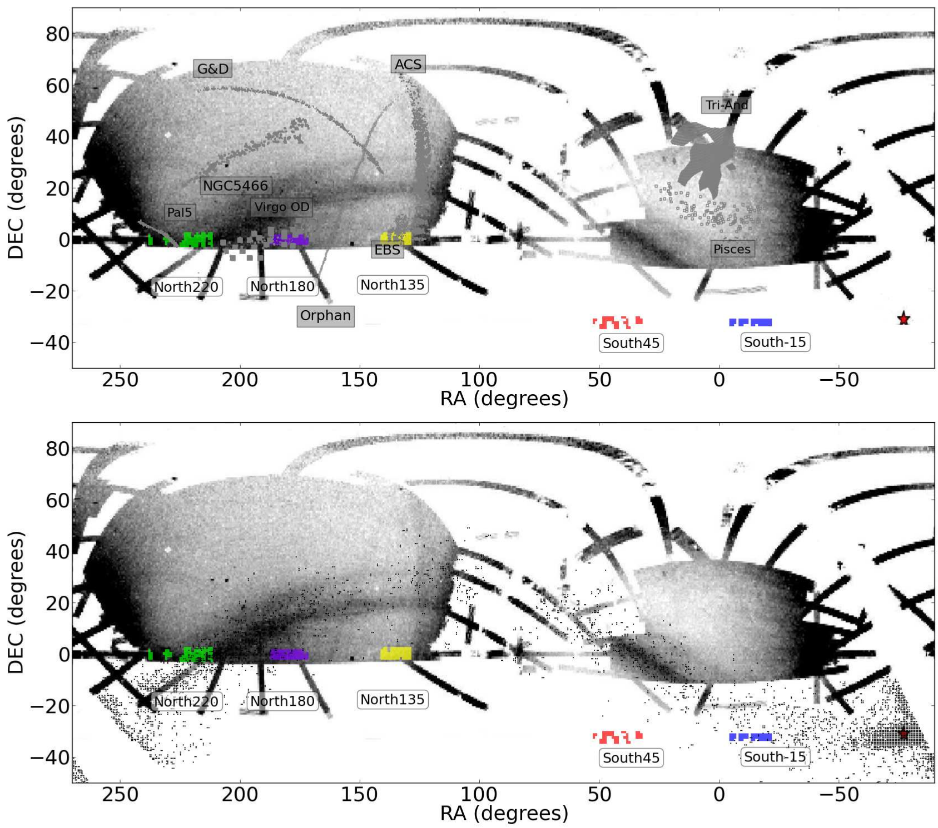

Figure 6.1: Top panel: equatorial map showing the KiDS DR-1 and DR-2 footprint (in colour) and several of the halo stellar streams (grey scale). Bottom panel: equatorial map showing the KiDS DR-1 and DR-2 footprint (in colour) together with the Sagittarius stream as seen by SDSS (background image) and by 2MASS (scattered black dots). The SDSS density map is from Koposov et al. (2012) while the 2MASS data are from Majewski et al. (2003). The red star indicates the position of the stream's progenitor, the Sagittarius dwarf galaxy.

Table 6.1: KiDS fields of view as shown in Figure 6.1. The table indicates the total area probed by KiDS DR-1 and DR-2 for each field and the a factor used to calcualte the kernel's bandwidth for the stellar density maps. Parameter a is a magic number chosen to optimize the granularity of the density maps.

Group	a	*Area* (deg^2)
KiDS-North220	4.8	29
KiDS-North180	6.6	37
KiDS-North135	5.4	37
KiDS-South45	3.6	14
KiDS-South-15	14.1	16

distance slices (from $[10, 15]$ kpc to $[40, 55]$ kpc) in two forms: i) scatterplots showing individual stars, and ii) density maps built with a k-Nearest Neighbours algorithm that uses a gaussian kernel with spatially variable bandwidth. The bandwidth is tailored to each KiDS field, and is calculated as $a/std(map)$, where a is a constant (see table 6.1) and $std(map)$ is the standard deviation of the stellar counts in that field at the specific distance range of each map. The density for each map is normalized over the mean density for that particular field and distance range, resulting in a pixel by pixel signal-to-background function.

On these maps we look for two things: first, we look for broad density gradients across the maps, as a sign of large substructures spanning several degrees in width and length. Second, we look for specific small overdensities spanning only a few degrees in width (if they are elongated) or in diameter (if they are rounded). We request these features to have high signal-to-background values and to fade out into more than one distance slice.

For the large gradients and structures, we look for a spatial overlap with known overdensities given that most of our continuous coverage is in the North fields (where SDSS has already probed the halo). This helps us identify the overdensities. We also produce magnitude (distance) vs RA maps for the North and the South fields as a way to recover again these features and trace their evolution along RA (Figures 6.12 to 6.15).

For the candidate small overdensities, we plot the individual CMD of the tile where each one is located and look for distinct main sequences or red clumps. A plot of the positions of just these stars in an equatorial map of the tile can then be used to assess whether this is a distinct object or a chance enhancement. Results of our analysis of the most promising overdensities are presented in Table 6.2).

6.3.2 Results

We identify large structures in all the KiDS fields except in KiDS-South45. In particular, Figure 6.12 and 6.13 show the Eastern Band Structure (Li et al. 2012, EBS) in KiDS-North135, the Virgo Overdensity (Bonaca et al. 2012b) in KiDS-North180 and both the Galactic disk and the Sagittarius stream in KiDS-

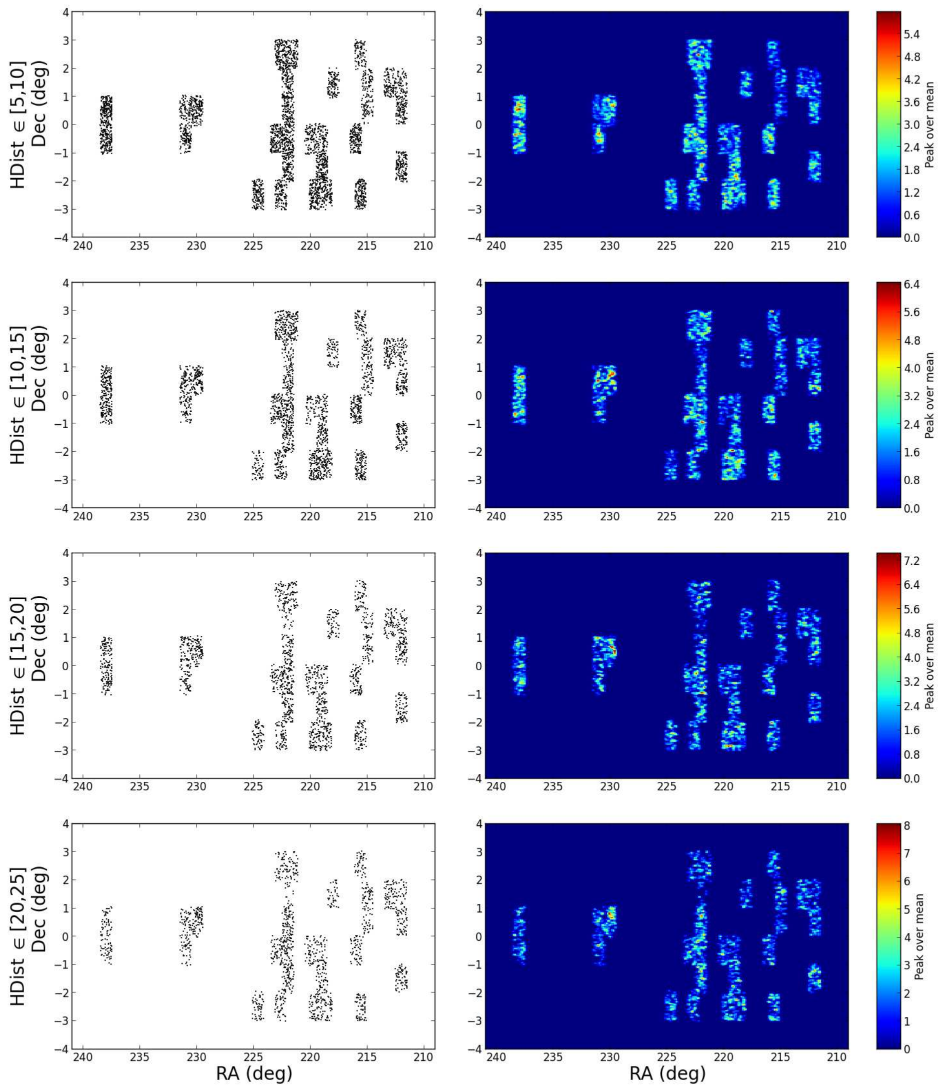

Figure 6.2: Stellar scatter maps and stellar density maps for the closest distance slices in field KiDS-North220.

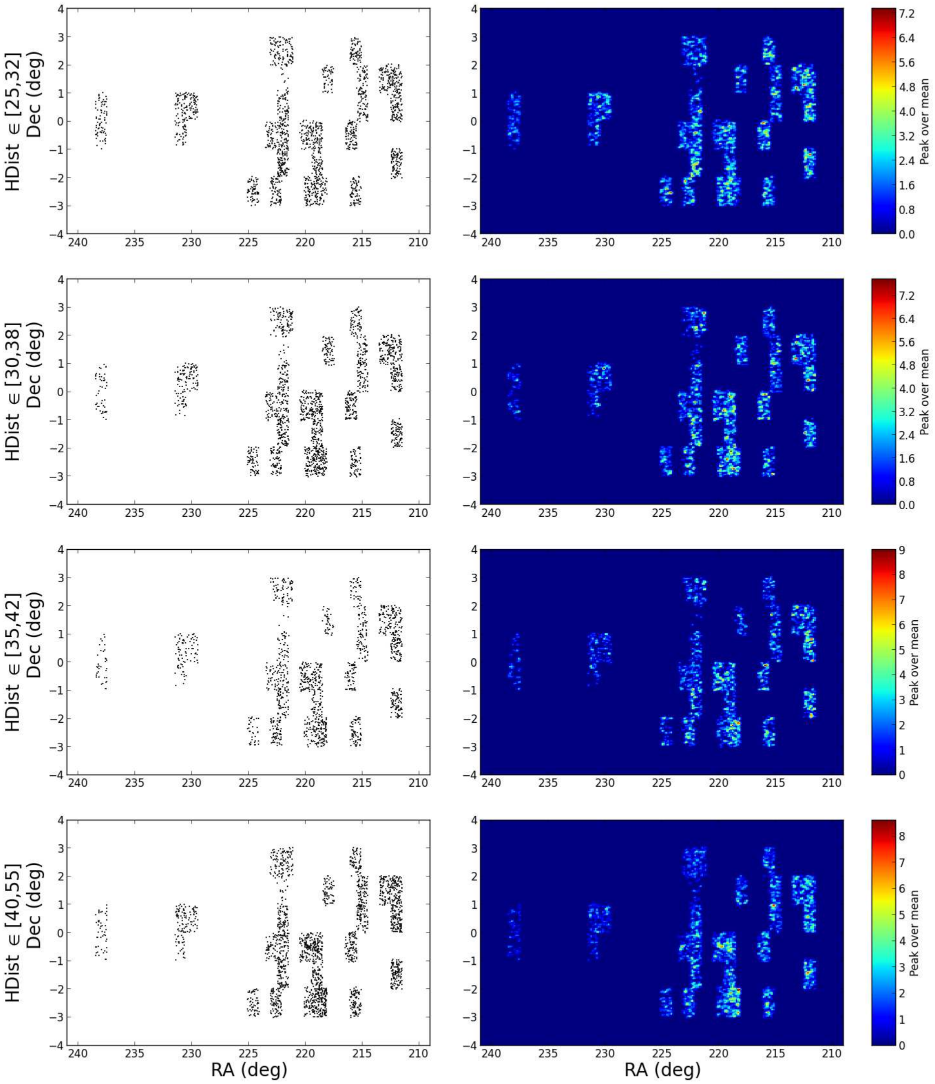

Figure 6.3: Stellar scatter maps and stellar density maps for the furthest distance slices in field KiDS-North220(continuation of Figure 6.2).

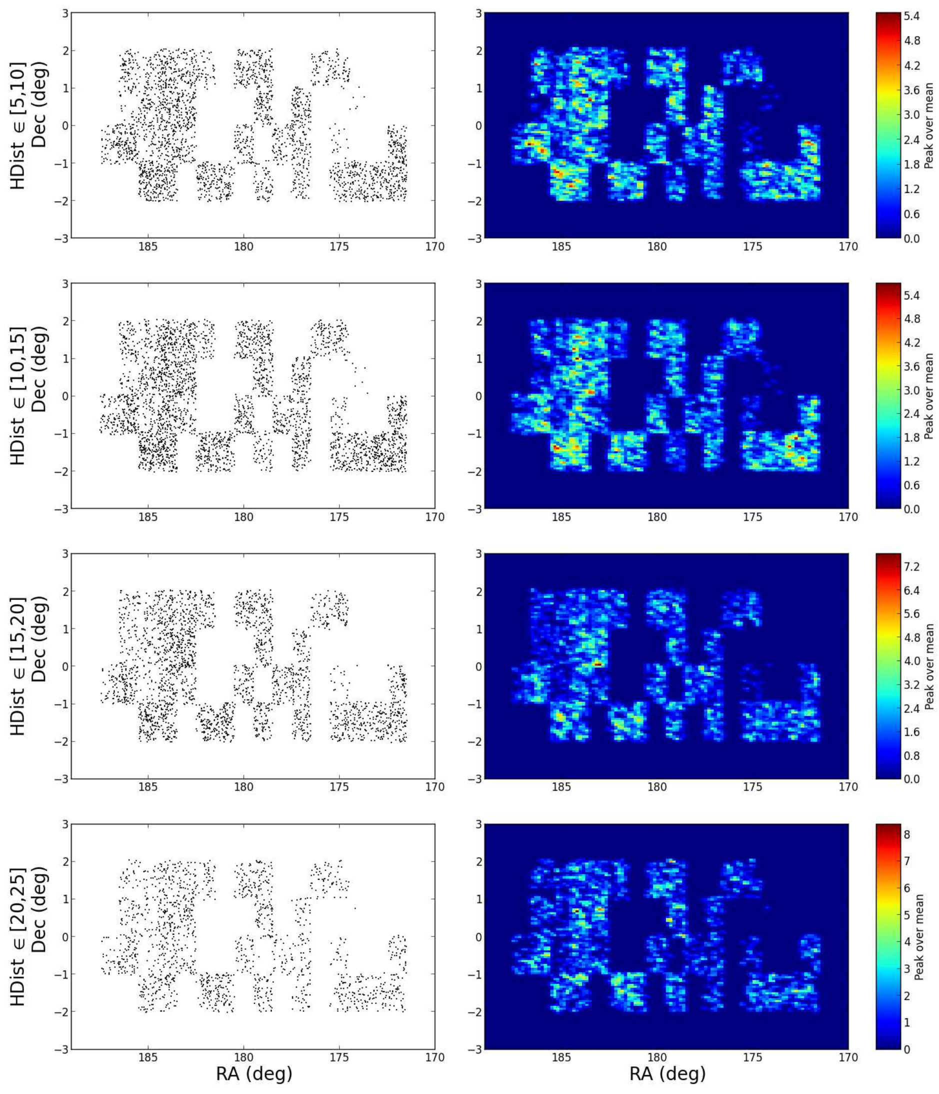

Figure 6.4: Stellar scatter maps and stellar density maps for the closest distance slices in field KiDS-North180.

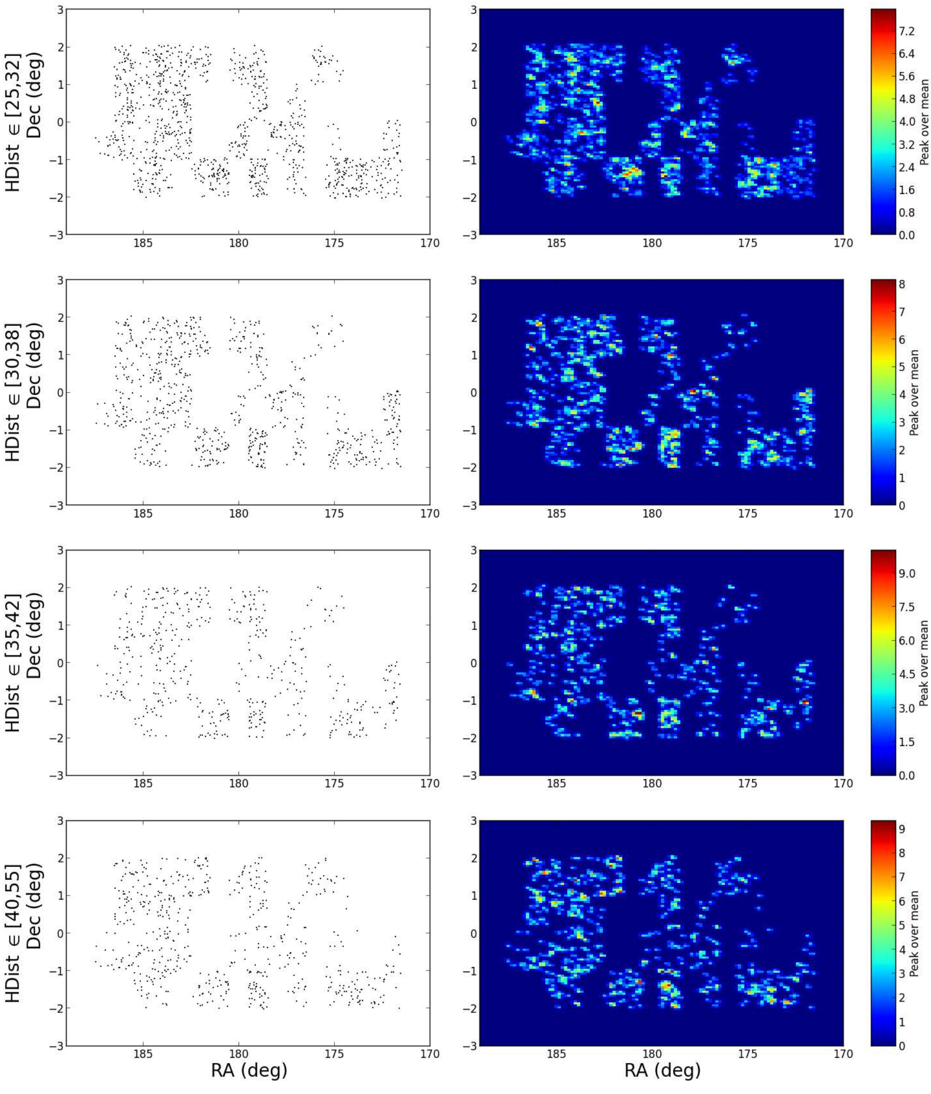

Figure 6.5: Stellar scatter maps and stellar density maps for the furthest distance slices in field KiDS-North180(continuation of Figure 6.4).

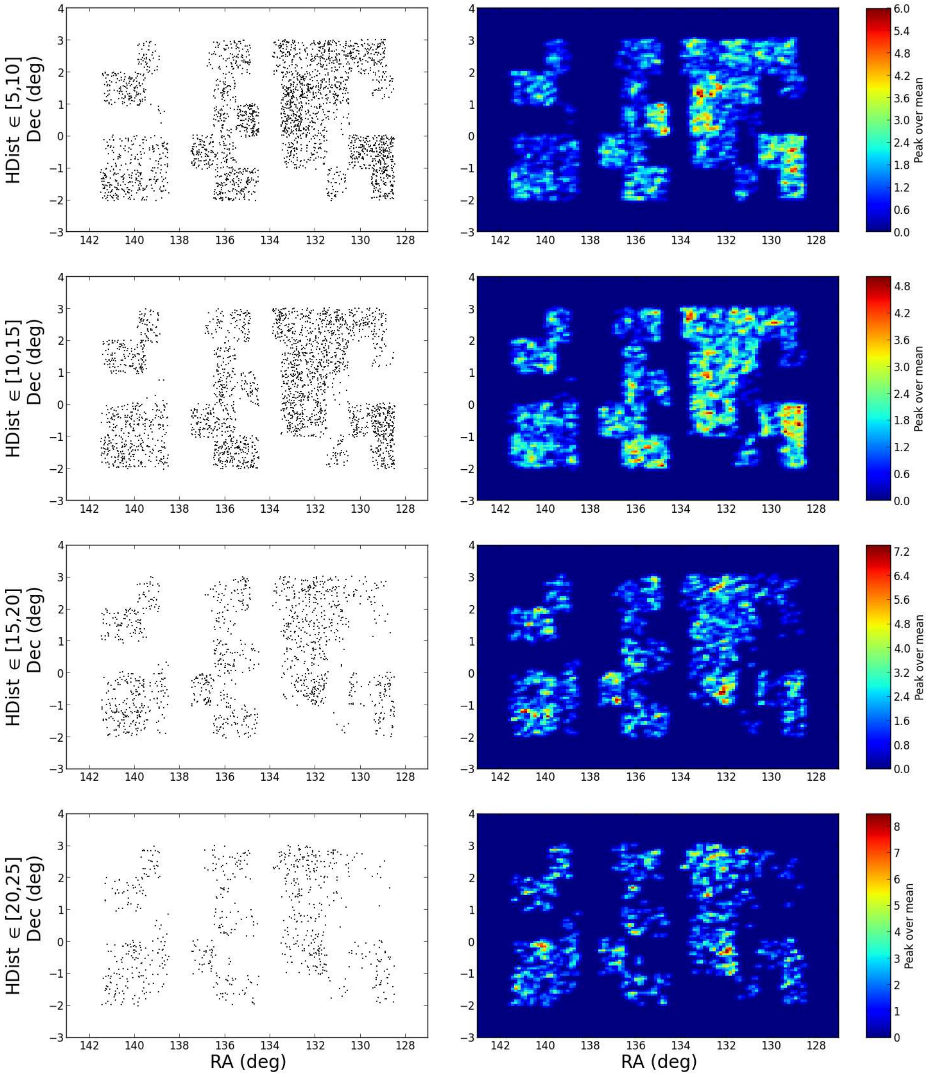

Figure 6.6: Stellar scatter maps and stellar density maps for the closest distance slices in field KiDS-North135.

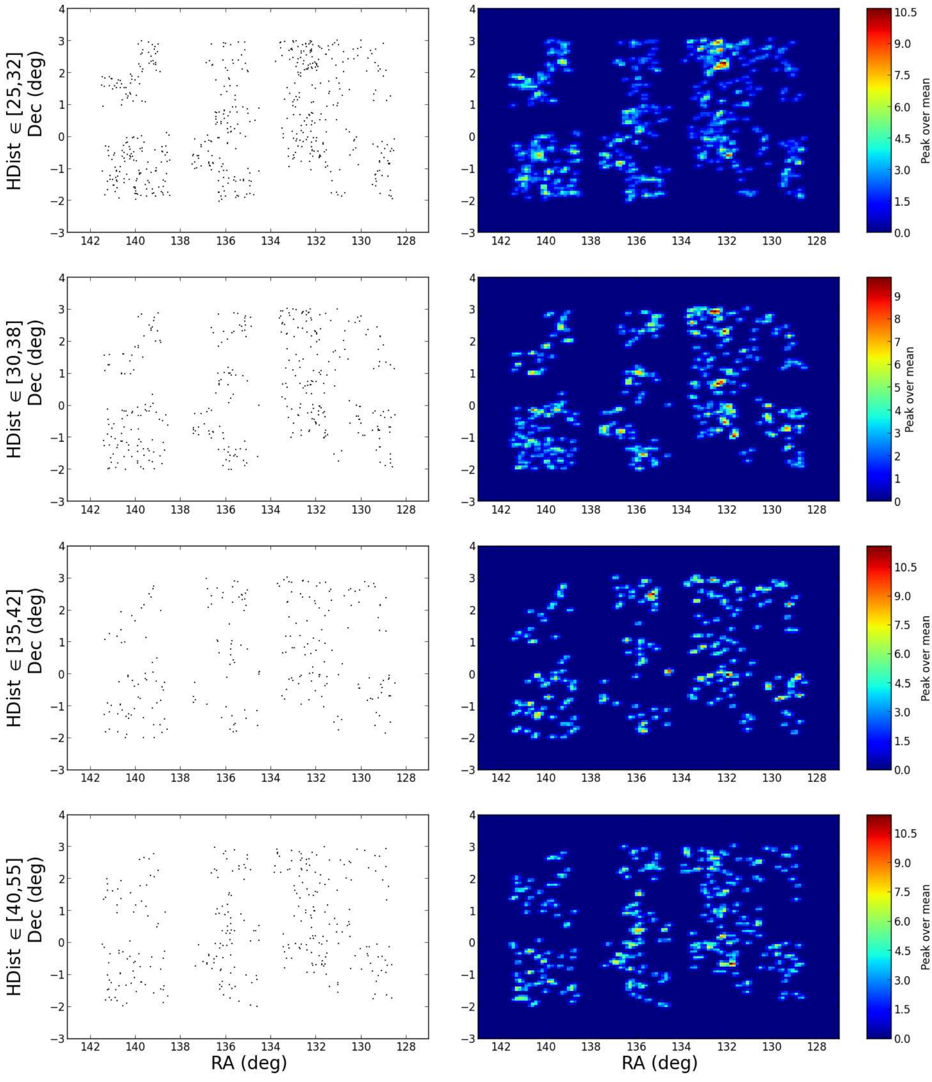

Figure 6.7: Stellar scatter maps and stellar density maps for the furthest distance slices in field KiDS-North135 (continuation of Figure 6.6).

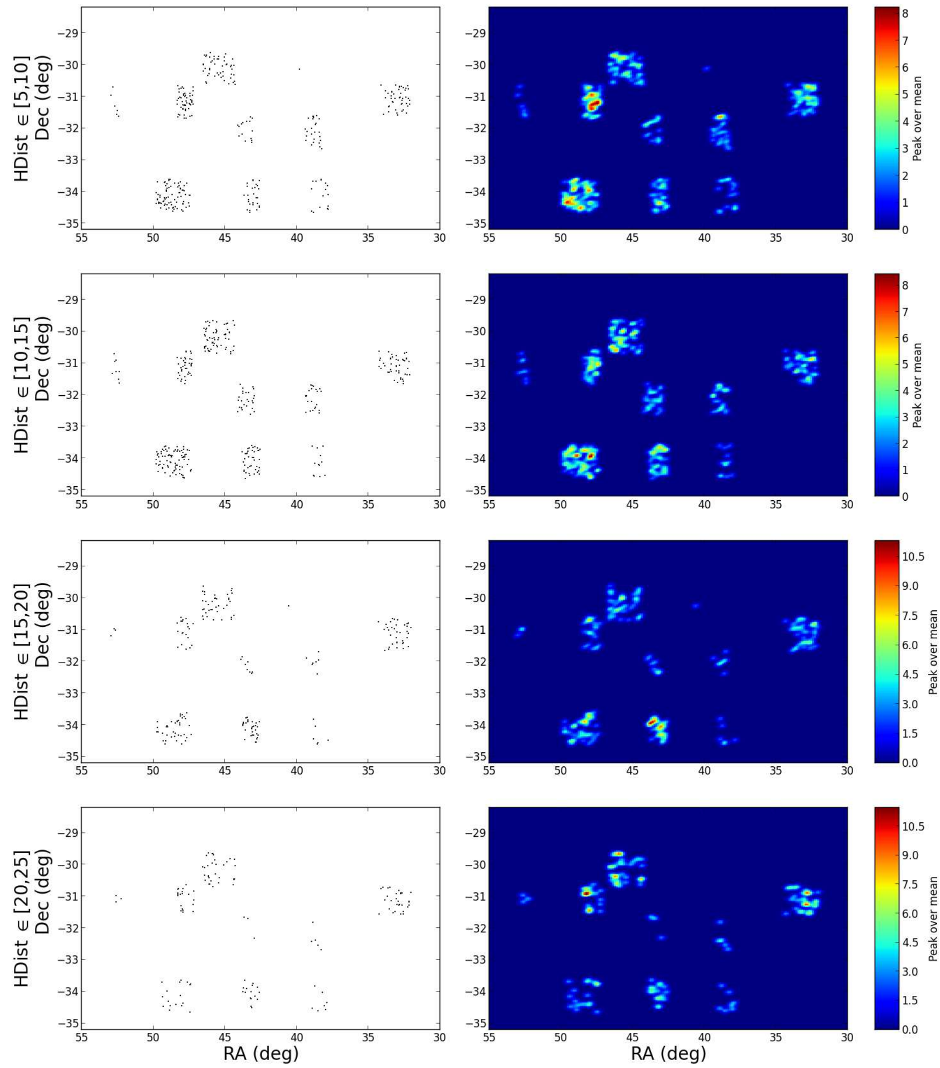

Figure 6.8: Stellar scatter maps and stellar density maps for the closest distance slices in field KiDS-South45.

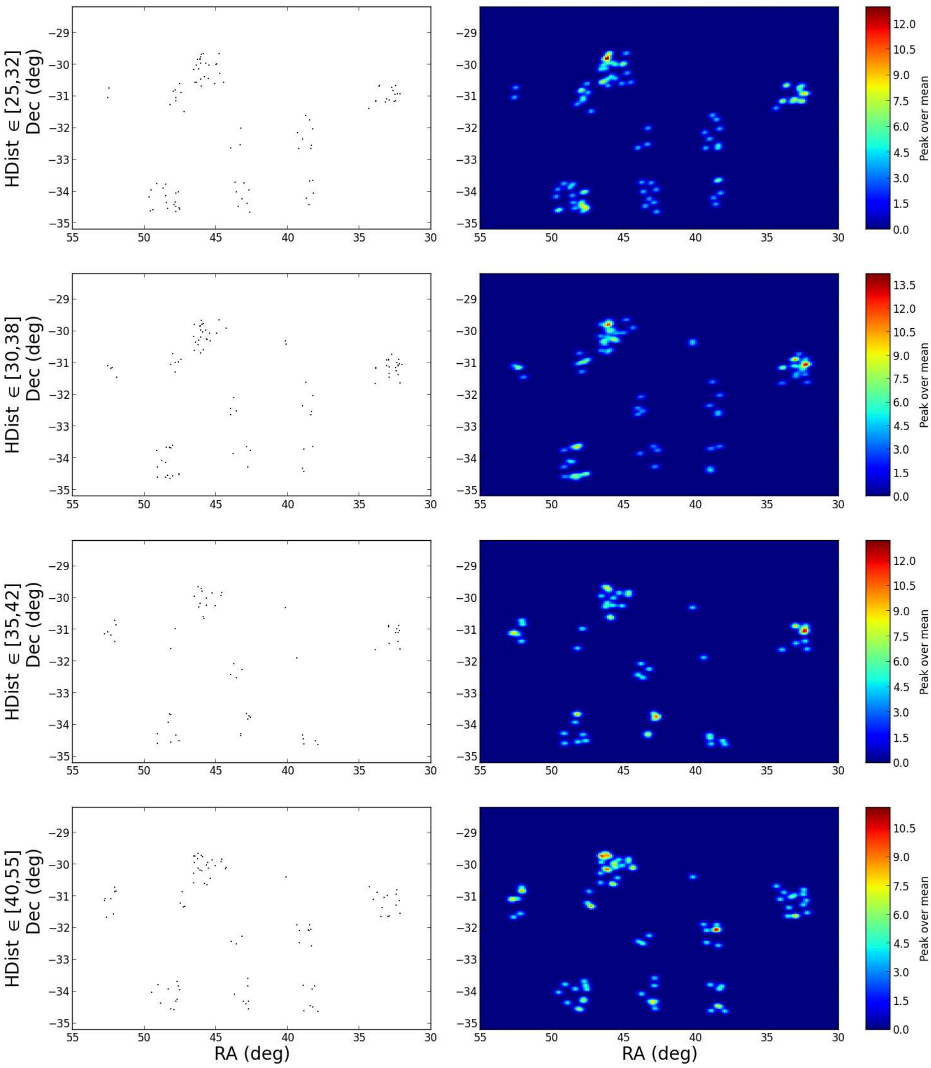

Figure 6.9: Stellar scatter maps and stellar density maps for the furthest distance slices in field KiDS-South45(continuation of Figure 6.8).

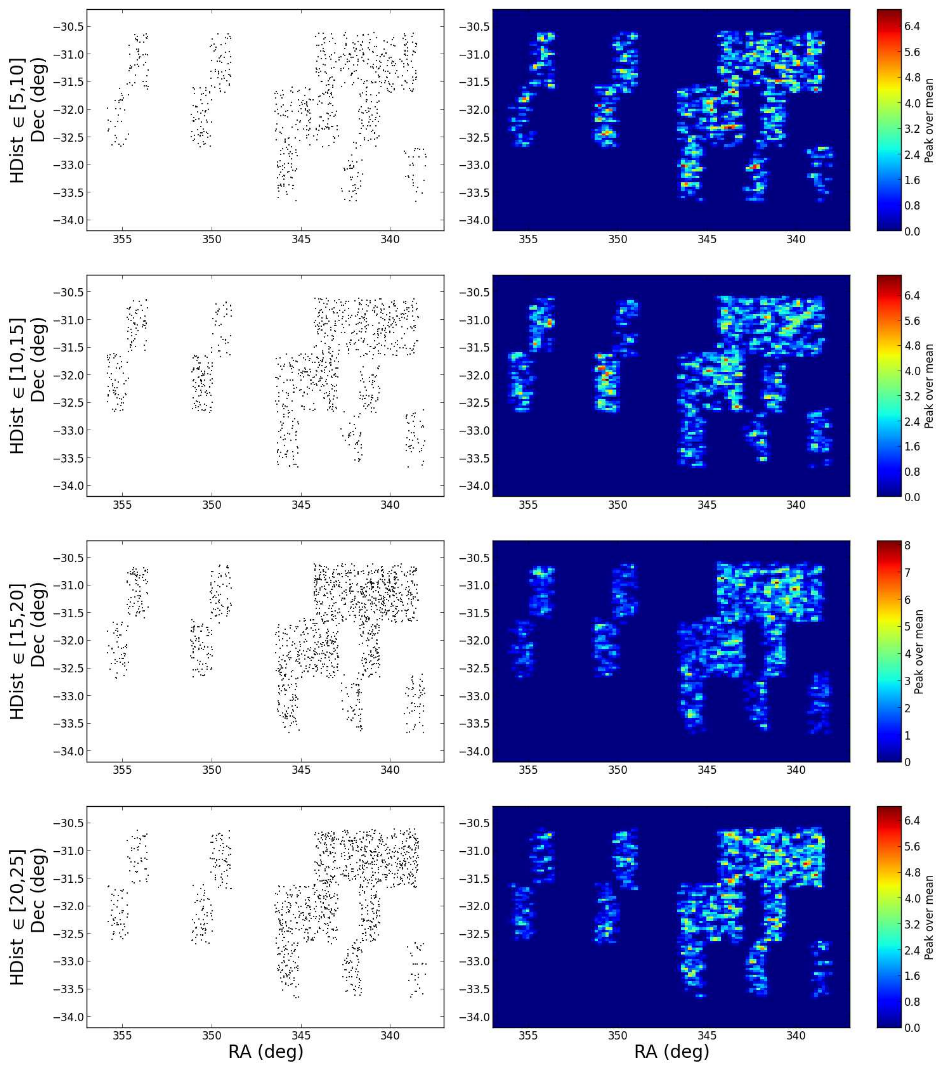

Figure 6.10: Stellar scatter maps and stellar density maps for the closest distance slices in field KiDS-South-15.

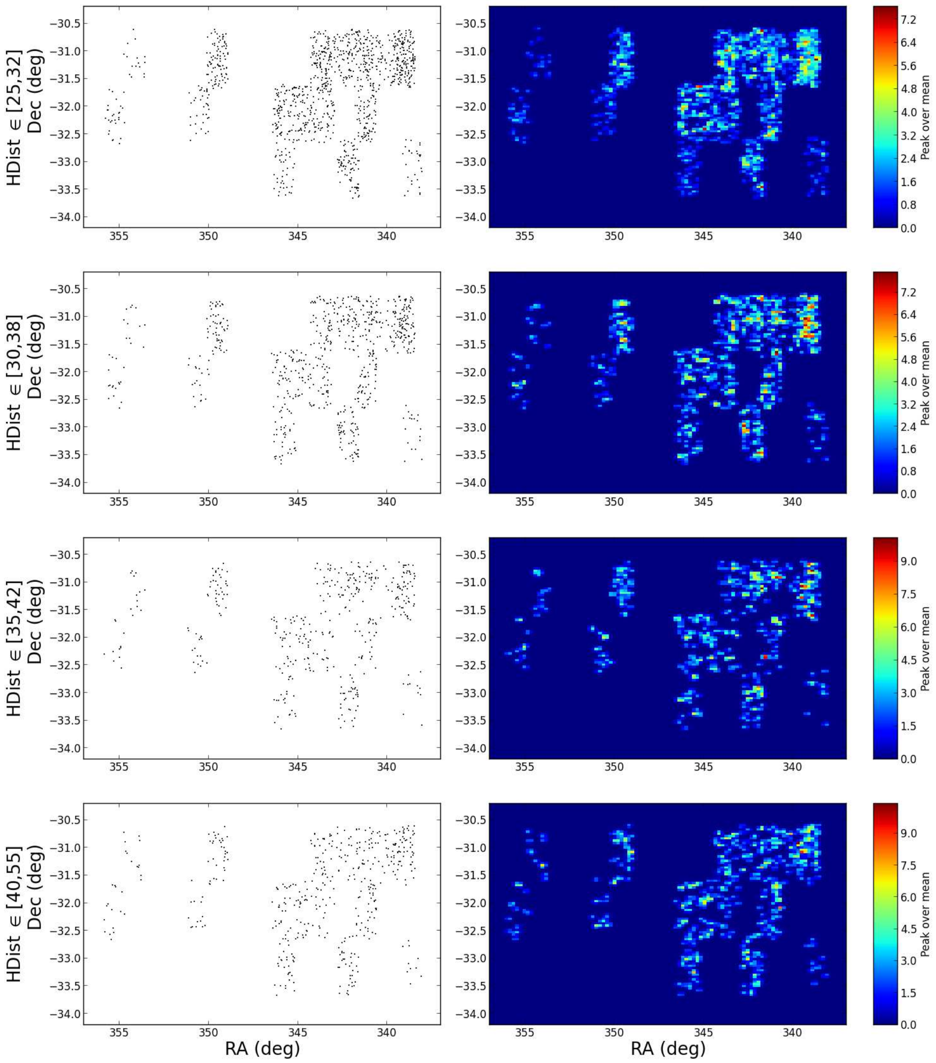

Figure 6.11: Stellar scatter maps and stellar density maps for the furthest distance slices in field KiDS-South-15(continuation of Figure 6.10).

North220. It is worth noting that the inner-halo or disk structures are more easily recognizable in the distance-RA maps than in the mag-RA maps, whereas the outer halo structures show the opposite effect. The reason for this is the logarithmic concentrating power of magnitudes in relation to distances as distances increase, which becomes very relevant when large volumes are probed and the average stellar densities decrease. Conversely, the same effect washes out short scale overdensities when these ones are located nearby.

In the KiDS-North220 field, the presence of disk stars is detected at least out to $12 - 15$ kpc. The Virgo Overdensity stretches out to 20 kpc in heliocentric distances and, in its western-most regions, possibly out to $25 - 30$ kpc. The EBS is mostly concentrated at under 15 kpc, with some potential debris extending further out to 20 kpc. The Sagittarius stream's nearMSTO stars overdensity in KiDS-North220 clearly peaks at $22.0 - 22.2$ mag in r but extends from ~ 21.6 to ~ 22.9, indicating a broad branch and possibly a dependence of distance with declination. Assuming an average absolute magnitude of $M_{r,TO} = 4.00$ for the MSTO of the Sagittarius stream (Pila-Díez et al. 2014), these magnitudes translate into a peak distance of 40 kpc and $[33, 60]$ kpc (soft) boundaries.

Figure 6.14 and 6.15 show the Sagittarius stream in KiDS-South-15, in agreement with its location on the 2MASS maps. At these latitudes, the stream sits at a distance between ~ 15 kpc and ~ 30 kpc, in agreement with the predictions of Law & Majewski (2010b) and Peñarrubia et al. (2010). Such a wide range of distances suggests the possible presence of two wraps (the leading and the trailing) or a quite thick branch in this region of the sky.

Among the small candidate overdensities, we identify one as a fragment of the Palomar 5 (Pal5) globular cluster tidal tails (Grillmair & Dionatos 2006a). The still patchy coverage of KiDS in the $RA > 225\,\text{deg}$ range unfortunately prevents us from fully tracing the stream. Nonetheless, we follow the procedure described above to analyse the CMD of this overdensity and demarcate the excess of stars within the tiles area. A clear main sequence and main sequence turnoff point are visible in the CMD corresponding to the tile centred at $(RA, Dec) = (230.0, 0.5)\,\text{deg}$ (left panel on Figure 6.16), and even a secondary main sequence turnoff point is located at fainter magnitudes. As discussed in Pila-Díez et al. (2014), these originate in the Pal5 tail and the underlying Sagittarius stream, respectively. We isolate the stars in the Pal5 tail's main sequence, and build a stellar density map of the tile specific to this substructure (right panel on Figure 6.16). This map nicely shows the Pal5 tail crossing the tile through its North-East quadrant.

For the rest of the small overdensities (Table 6.2) we follow the same procedure. From their CMD and stamp maps we find that these are either i) spurious enhancements in the distance/magnitude-sliced maps (this is, RC/nearMSTO-colour overdensities in the CMD without the companion RGB/main sequence overdensity), or ii) apparent main sequences in the CMD but without a coherent spatial feature in the stamp map (meaning that, when plotting different colour-magnitude sections of the apparent main sequence on the stamp map, they popu-

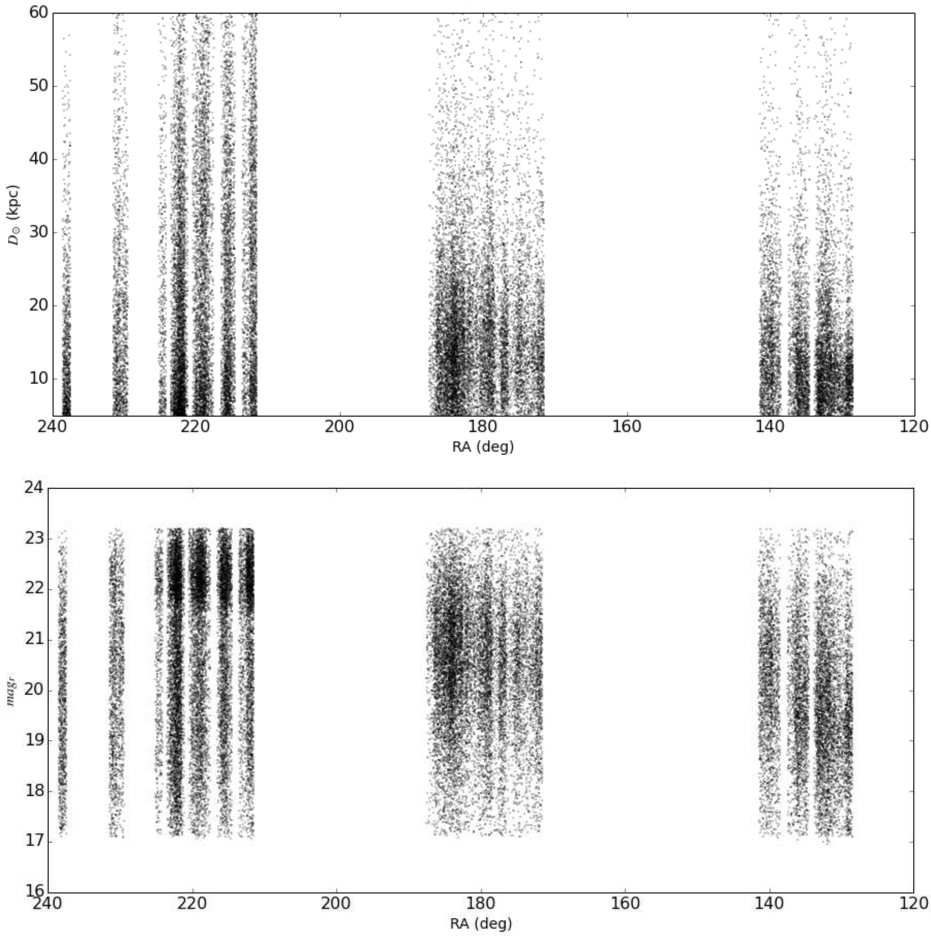

Figure 6.12: Distance vs RA (top) and magnitude vs RA (bottom) scatter maps for the nearMSTO stars in the KiDS Northern fields. Both the disk and large halo structures like the Sagittarius stream, the Virgo Overdensity and the EBS are visible. This figure illustrates that the nearby structures are more easily recognizable in the distance space than the far structures, whereas the far structures are more easily recognizable in the magnitude space. This is due to the logarithmic concentrating power of magnitudes in relation to distances.

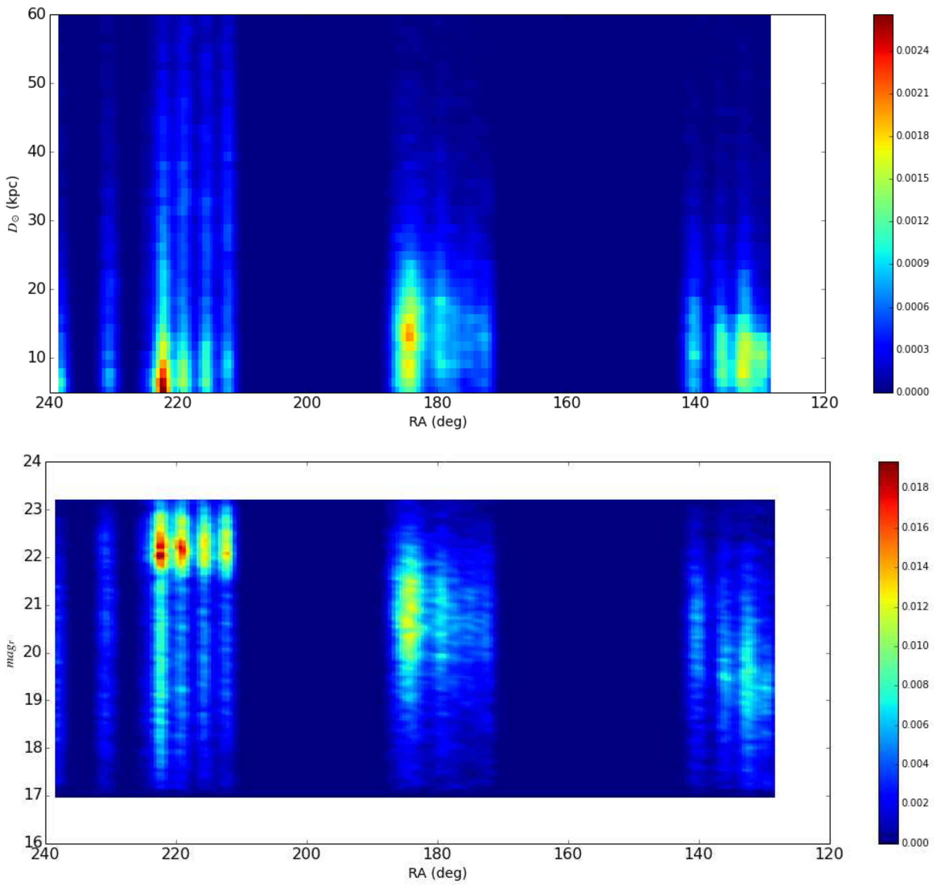

Figure 6.13: Same as in Figure 6.12 but showing the stellar density map instead of the stellar counts map. The density has been calculated with a gaussian kernel of variable bandwidth.

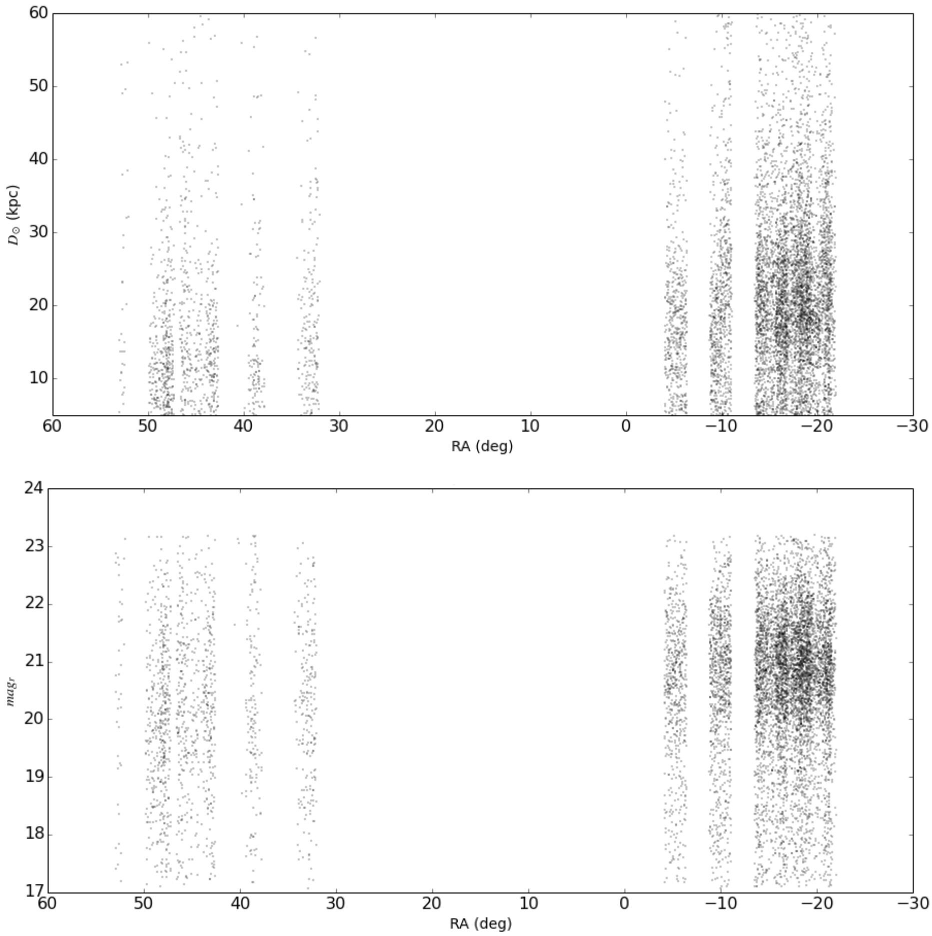

Figure 6.14: Distance vs RA (top) and magnitude vs RA (bottom) scatter maps for the nearMSTO stars in the KiDS Southern fields. The Sagittarius stream is visible in the eastern part of the field.

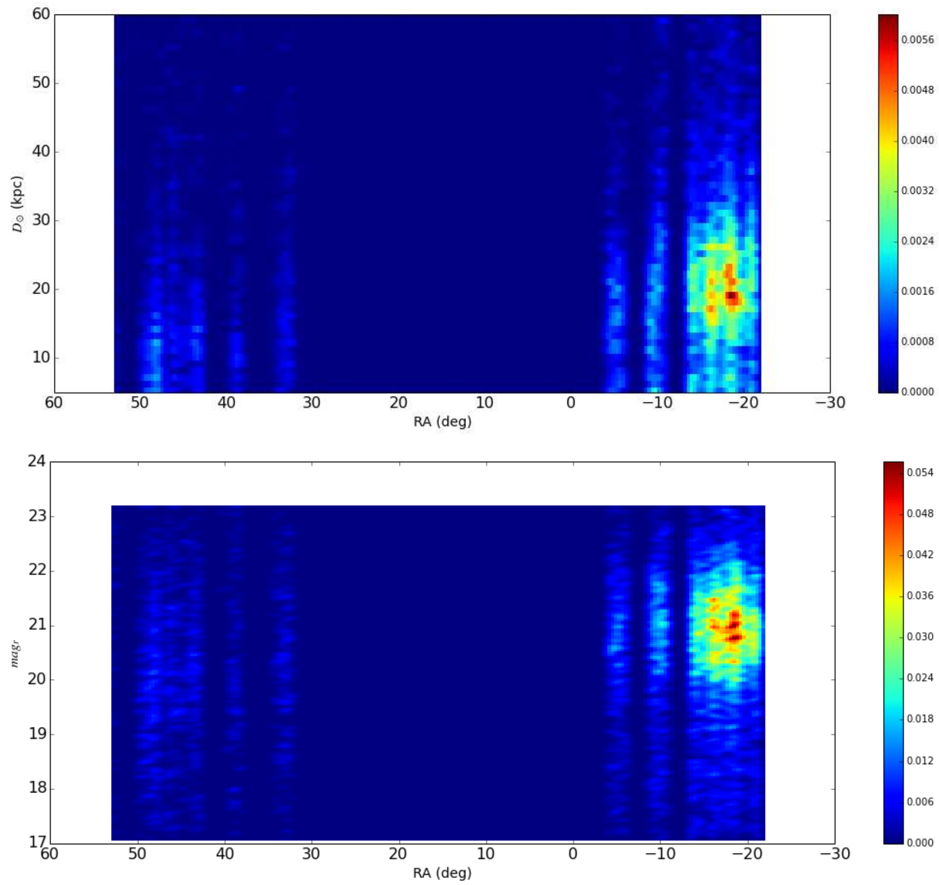

Figure 6.15: Same as in Figure 6.14 but showing the stellar density map instead of the stellar counts map.The density has been calculated with a gaussian kernel of variable bandwidth.

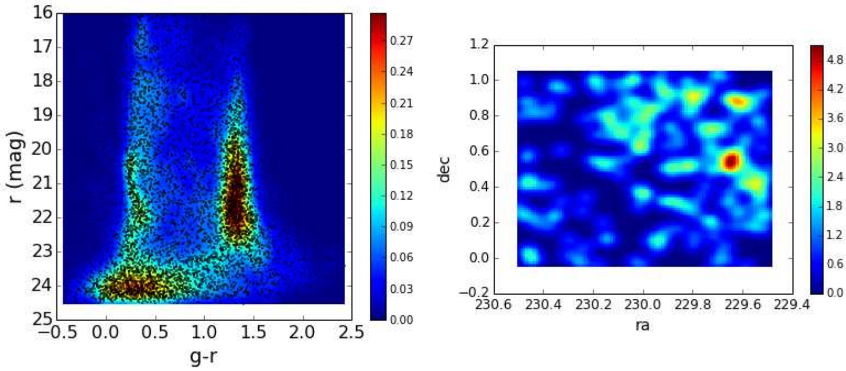

Figure 6.16: CMD (left) and stellar density map (right) for the stars in the main sequence of the CMD (right), pointing centered at $(RA, Dec) = (230.0, 0.5)$ deg. The main sequence at $20.0 < r < 22.0$ represents the Palomar 5 stream. The secondary main sequence visible at $r \approx 23$ is the Sagittarius stream.

Table 6.2: Potential small overdensities identified in the distance-sliced/magnitude-sliced nearMSTO or RC density maps. The table indicates the central coordinates of the tile where each was identified, tags them and provides a diagonisis (true or false positive).

Overdensity	Field	RA_{tile} (deg)	Dec_{tile} (deg)	positive
Pal5	KiDS-North220	230.0	0.5	true
A	KiDS-North180	179.0	-0.5	false
B	KiDS-North135	135.0	0.5	false
C	KiDS-North135	132.0	-0.5	false
D	KiDS-South45	47.8	-31.2	false
E	KiDS-South-15	350.6	-32.1	false

late different regions of the tile). Examples for the two types of cases are provided in Figures 6.17 and 6.18, respectively, corresponding to overdensities A and E. We conclude that all A to E overdensities are false positive halo substructures.

6.4 Discussion

The methods used in this work are technically robust (k-Nearest Neighbours, CMDs, distance or magnitude slicing, colour-colour star selection) and their effectivity for the halo has been amply tested in the literature. Indeed we are able to recover large known halo structures and also a fragment of the Palomar 5 tidal tails.

Therefore we associate the lack of a new discovery in the KiDS DR1/2 data to the small sky coverage that KiDS has so far achieved in areas of the sky not

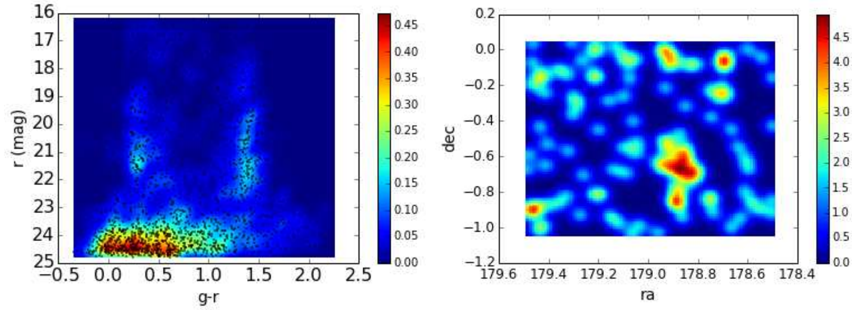

Figure 6.17: CMD (left) and stellar density map (right) corresponding to the pointing centered at $(RA, Dec) = (179.0, -0.5)$ deg (labelled as A in Table 6.2). The stellar density map contains the stars in the apparent main sequence of the whole pointing (not shown), and the CMD is built of the stars located in the vicinity of the overdensity at $(RA, Dec) \approx (178.9, -0.7)$ deg. The lack of a main sequence and an RGB on this CMD indicates that this overdensity in nearMSTO stars is a spurious enhancement and, therefore, is a false positive. Similar analysis on weaker spatial overdensities in this pointing lead to conclude that there is no localized main sequence in this pointing.

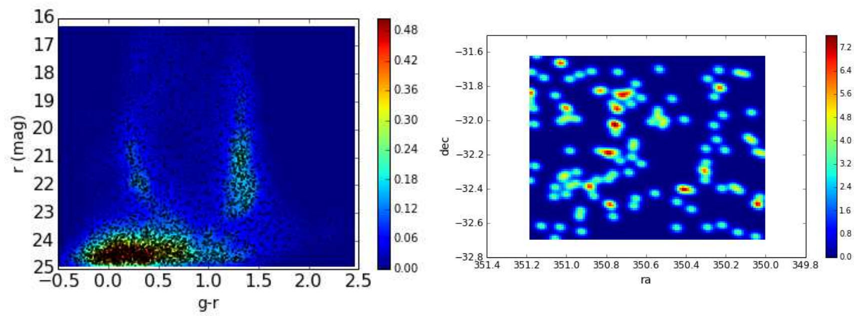

Figure 6.18: CMD (left) and stellar density map for the stars in the main sequence of the CMD (right). They correspond to the pointing centered at $(RA, Dec) = (350.6, -32.1)$ deg and to the overdensity labelled as E in Table 6.2. The lack of a coherent spatial feature indicates this is a false polsitive.

probed yet by other surveys. In particular, in the KiDS' northern fields there is a total overlap with the footprint of the latest SDSS data releases, and there was originally a $\sim 80\%$ overlap planned. Of the current $133\,\mathrm{deg}^2$ scanned by KiDS DR-1 and DR-2 in the four bands, only 23% belongs to the southern hemisphere. This limits KiDS current chances of detecting new globular clusters or satellite galaxies, and limits its ability to detect and trace weak streams.

Based both on the claims of a fundamental plane of satellite galaxies (Palma et al. (2002b), Zentner et al. (2005), Pawlowski et al. (2012)) and on the possibility of such a fundamental plane being probed wrong, but based mainly on the satellite population in the northern sky, the number of satellite galaxies expected to inhabit the southern sky is high. Furthermore the recent results by DES and ATLAS show good prospects, and do not suggest a fundamental asymmetry in the density of satellites between the northern and southern Galactic hemispheres. Given the current estimates for the Galactic satellite luminosity function (Koposov et al. 2008) and KiDS unprecedented power to probe faint objects, the prospects for KiDS are particularly good at the faint end. Therefore there is no reason for discouragement and future data releases of KiDS should uncover new satellites and stellar debris.

6.5 Conclusions

The Kilo Degree Survey is currently mapping $1500\,\mathrm{deg}^2$ of the sky at an unprecedented depth among large area surveys. Its good image quality, seeing constraints and multi-colour photometry make it particularly suited to explore the Galactic halo in depth. It targets both the North and the South Galactic hemispheres, overlapping with SDSS and ATLAS in each region respectively, but probing an average of two magnitudes deeper than any of the two surveys in any of the four photometric filters. The PSF-homogenization that we carry out allows us to accurately separate stars from galaxies, reaching a stellar magnitude limit of $mag_r = 23.1$ without significant galaxy contamination. This allows us to properly exploit main sequence turnoff point stars out to large heliocentric distances (~ 60 kpc).

In this work we present magnitude-sliced or distance-sliced maps for photometrically selected red clump stars and near main sequence turnoff point stars. We identify broad halo structures such as the Sagittarius stream, the Virgo Overdensity and the Eastern Band Structure in the northern hemisphere, and the Sagittarius stream in the southern hemisphere. In the northern hemisphere we also identify the disk stars at longitudes and latitudes neighbouring the Galactic centre. We trace these features in distance space and magnitude space and report heliocentric distances compatible with previous works.

We also identify in these distance/magnitude-sliced maps a number of small overdensities potentially representative of halo substructure. Of the seven identifications, we recognize one as a piece of the Palomar 5 tidal tails. The rest are classified as false positives after close inspection of their CMDs and the spatial distribution of any CMD overdensities.

The Kilo Degree Survey is promising in the search for small, sparse and faint substructure, given both its technical capabilities and the fact that it is probing uncharted halo territory in the Southern hemisphere. The current methodology presented in this chapter, together with state-of-the-art matched-filter algorithms, should suffice to identify new substructure in the halo once the spatial coverage of KiDS reaches a more mature stage and allows for more lines of sight (to detect new overdensities) and their spatial continuous follow-up.